

# Stacked quantum Ising systems and quantum Ashkin-Teller model

Davide Rossini<sup>1</sup> and Ettore Vicari<sup>2</sup>

<sup>1</sup>*Dipartimento di Fisica dell'Università di Pisa and INFN, Largo Pontecorvo 3, I-56127 Pisa, Italy*

<sup>2</sup>*Dipartimento di Fisica dell'Università di Pisa, Largo Pontecorvo 3, I-56127 Pisa, Italy*

(Dated: January 28, 2026)

We analyze the quantum states of an isolated composite system consisting of two stacked quantum Ising (SQI) subsystems, coupled by a local Hamiltonian term that preserves the  $\mathbb{Z}_2$  symmetry of each subsystem. The coupling strength is controlled by an intercoupling parameter  $w$ , with  $w = 0$  corresponding to decoupled quantum Ising systems. We focus on the quantum correlations of one of the two SQI subsystems,  $\mathcal{S}$ , in the ground state of the global system, and study their dependence on both the state of the weakly-coupled complementary part  $\mathcal{E}$  and the intercoupling strength. We concentrate on regimes in which  $\mathcal{S}$  develops critical long-range correlations. The most interesting physical scenario arises when both SQI subsystems are critical. In particular, for identical SQI subsystems, the global system is equivalent to the quantum Ashkin-Teller model, characterized by an additional  $\mathbb{Z}_2$  interchange symmetry between the two subsystem operators. In this limit, one-dimensional SQI systems exhibit a peculiar critical line along which the length-scale critical exponent  $\nu$  varies continuously with  $w$ , while two-dimensional systems develop quantum multicritical behaviors characterized by an effective enlargement of the symmetry of the critical modes, from the actual  $\mathbb{Z}_2 \oplus \mathbb{Z}_2$  symmetry to a continuous  $O(2)$  symmetry.

## I. INTRODUCTION

Any subsystem of an isolated quantum system made up of multiple components, such as quantum particles in a gas or quantum spins on a lattice, can be seen as an open system in contact with an effective bath (i.e., the remainder of the global system). In this respect, one may study the nonunitary quantum dynamics of the subsystem as if it were subject to the interaction with some environment, while the global system evolves unitarily [1, 2]. Several paradigmatic and relatively simple composite models have been considered in the literature. We mention, for example, the so-called *central-spin* models, where one or few qubits are globally coupled to an environmental many-body system (see, e.g., Refs. [3–24]), models in which a single spin is locally coupled to a many-body environment [7, 25–27], *sunburst* spin models, where sets of isolated qubits are locally coupled to a many-body system [28–32], *stacked* quantum many-body systems [33–36], etc. The quantum correlations and decoherence properties of the subsystems turn out to depend crucially on the global features of their state, whether a given subsystem is in an ordered or a disordered quantum phase, or it is close to a quantum critical point, where large-scale critical correlations develop [37–39].

To further investigate the quantum dynamics of composite systems, we consider stacked quantum Ising (SQI) systems, locally and homogeneously coupled, as sketched in Fig. 1 for a one-dimensional (1D) setup, as theoretical laboratories. One of the two subsystems represents the part  $\mathcal{S}$  under observation, while the other plays the role of the environment  $\mathcal{E}$ . Specifically, we study the case in which the subsystems are locally coupled by Hamiltonian terms that do not break the  $\mathbb{Z}_2$  symmetries of each SQI subsystem, such as a local coupling proportional to the product of their transverse spin operators. The Hamiltonian parameters of the two subsystems may

differ, so that weakly coupled  $\mathcal{S}$  and  $\mathcal{E}$  can effectively lie in different quantum phases. We analyze the quantum correlations of  $\mathcal{S}$  within the ground state of the global system  $\mathcal{S} \oplus \mathcal{E}$ , focusing on regimes in which  $\mathcal{S}$  develops critical long-range correlations, and study their dependence on the state of the weakly-coupled complementary part  $\mathcal{E}$  and on the intercoupling strength. By means of renormalization-group (RG) arguments and extensive numerical simulations based on the density-matrix RG (DMRG) algorithm [40], we investigate how a weak interaction between  $\mathcal{S}$  and  $\mathcal{E}$  affects the scaling behaviors of  $\mathcal{S}$ , close to quantum critical regimes in the limit of zero temperature. We mostly analyze 1D SQI systems, and eventually extend the discussion to higher-dimensional models, in particular to two-dimensional (2D) SQI systems.

It is worth noting that one may also consider SQI systems with different types of local intercoupling, such as that considered in Ref. [36], where the interaction term between  $\mathcal{S}$  and  $\mathcal{E}$  is proportional to the product of the longitudinal spin variables. In that case, the global symmetry is altered: the intercoupling breaks the individual  $\mathbb{Z}_2$  symmetries of the Ising subsystems, leaving only a global residual  $\mathbb{Z}_2$  symmetry. Substantial differences emerge when comparing the critical behaviors of SQI

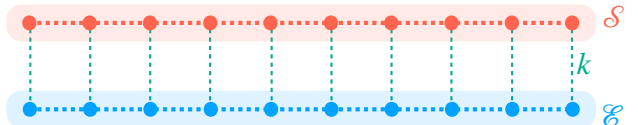


FIG. 1: Sketch of a system made of two SQI chains, weakly coupled by local and homogeneous interactions controlled by a single, generic, parameter  $k$ . One of the chains represents the subsystem  $\mathcal{S}$ , while the other one plays the role of the environment  $\mathcal{E}$ .

models that preserve or break the original symmetries of the decoupled subsystems. Nevertheless, in both cases the critical behavior developed within  $\mathcal{S}$  depends crucially on the state of  $\mathcal{E}$ , whether it is critical or far from criticality.

The paper is organized as follows. In Sec. II we introduce the 1D SQI model studied in this work and define some observables defined within the subsystem  $\mathcal{S}$ . In Sec. III we discuss the critical behavior of  $\mathcal{S}$ , when the environment  $\mathcal{E}$  is weakly coupled and far from criticality, being effectively in a disordered or ordered state. In Sec. IV we focus on the most interesting case in which both subsystems develop critical correlations, and present a numerical analysis of the finite-size scaling (FSS) behavior in the limit of equal SQI subsystems, which becomes equivalent to the quantum Ashkin-Teller (QAT) model. In Sec. V we extend our discussion to higher dimensions, and in particular to 2D SQI models, arguing the emergence of a peculiar multicritical behavior characterized by an effective extension of the global symmetry. Finally, in Sec. VI we summarize and draw our conclusions. In App. A we provide some details on our DMRG simulations and on their accuracy, while in App. B we report some results for the behavior of critical two-point correlation functions of 1D quantum Ising chains, obtained by conformal field theory (CFT).

## II. STACKED QUANTUM ISING CHAINS

### A. The model

We consider 1D SQI models coupled by local interactions which preserve their  $\mathbb{Z}_2$  symmetry [37–39], as described by the Hamiltonian

$$\hat{H} = \hat{H}_\sigma + \hat{H}_\tau + \hat{H}_w, \quad (1)$$

where

$$\hat{H}_\sigma = -J \sum_{x=-\ell}^{\ell-1} \hat{\sigma}_x^{(1)} \hat{\sigma}_{x+1}^{(1)} - g \sum_{x=-\ell}^{\ell} \hat{\sigma}_x^{(3)}, \quad (2a)$$

$$\hat{H}_\tau = -J_e \sum_{x=-\ell}^{\ell-1} \hat{\tau}_x^{(1)} \hat{\tau}_{x+1}^{(1)} - g_e \sum_{x=-\ell}^{\ell} \hat{\tau}_x^{(3)}, \quad (2b)$$

$$\hat{H}_w = -w \left[ \sum_{x=-\ell}^{\ell-1} \hat{\sigma}_x^{(1)} \hat{\sigma}_{x+1}^{(1)} \hat{\tau}_x^{(1)} \hat{\tau}_{x+1}^{(1)} + \sum_{x=-\ell}^{\ell} \hat{\sigma}_x^{(3)} \hat{\tau}_x^{(3)} \right]. \quad (2c)$$

Here,  $\hat{\sigma}_x^{(k)}$  and  $\hat{\tau}_x^{(k)}$  are two sets of Pauli matrices ( $k = 1, 2, 3$ ) on each site  $x$ , with  $-\ell \leq x \leq \ell$ . We generally consider systems in which each of the two chains has open boundary conditions (OBC) and is composed of  $L = 2\ell + 1$  sites. In the following, we also set  $\hbar = 1$ .

The model (1)-(2) has a global  $\mathbb{Z}_2 \oplus \mathbb{Z}_2$  symmetry for generic values of the parameters  $J, g, J_e, g_e$ , and  $w$ , com-

bining the two independent parity symmetries

$$\hat{\sigma}_x^{(1)} \rightarrow -\hat{\sigma}_x^{(1)}, \quad \hat{\sigma}_x^{(3)} \rightarrow \hat{\sigma}_x^{(3)}, \quad (3a)$$

$$\hat{\tau}_x^{(1)} \rightarrow -\hat{\tau}_x^{(1)}, \quad \hat{\tau}_x^{(3)} \rightarrow \hat{\tau}_x^{(3)}. \quad (3b)$$

When  $J = J_e$  and  $g = g_e$ , the global symmetry extends to a further interchange  $\mathbb{Z}_2$  symmetry

$$\hat{\sigma}_x \leftrightarrow \hat{\tau}_x. \quad (4)$$

In the latter case, we recover the 1D QAT model [41–47], whose critical properties are related to those of the 2D classical Ashkin-Teller (CAT) model [48, 49] by a quantum-to-classical mapping.

When the interaction between the SQI chains vanishes (i.e., when  $w = 0$ ), one recovers two decoupled quantum Ising chains, with Hamiltonians  $\hat{H}_\sigma$  and  $\hat{H}_\tau$ , respectively. The single chain undergoes a zero-temperature continuous quantum transition at a critical value  $g_{\mathcal{I}}$  of the transverse field,

$$g_{\mathcal{I}} = J, \quad (5)$$

see, e.g., Refs. [38, 39, 50]. The corresponding quantum critical behavior belongs to the 2D Ising universality class. The deviation  $r \equiv g - g_{\mathcal{I}}$  represents the leading RG perturbation which preserves the  $\mathbb{Z}_2$  symmetry. Its RG dimension is  $y_r = 1/\nu_{\mathcal{I}} = 1$ , so that the length scale  $\xi$  of the critical modes behaves as  $\xi \sim |g - g_{\mathcal{I}}|^{-\nu_{\mathcal{I}}}$ . The dynamic exponent, controlling the vanishing of the gap  $\Delta \sim \xi^{-z}$  at the transition point, is  $z = 1$ . The RG dimension  $y_\phi$  of the longitudinal spin operator  $\hat{\sigma}_x^{(1)}$ , associated with the order parameter at the Ising transition, is given by  $y_\phi = \eta/2 = 1/8$ , where  $\eta = 1/4$  is the critical exponent characterizing the spatial decay of the critical correlations of  $\hat{\sigma}_x^{(1)}$ . For any  $g < g_{\mathcal{I}}$ , the presence of a homogeneous longitudinal field  $h$  coupled to the spin operator  $\hat{\sigma}_x^{(1)}$  drives first-order quantum transitions at  $h = 0$ . In particular, for  $|h| \rightarrow 0$ , the magnetized states  $|+\rangle$  and  $|-\rangle$  along the longitudinal direction are the ground states of the system for  $h > 0$  and  $h < 0$ , respectively, giving rise to a discontinuous infinite-volume longitudinal magnetization  $m_0$ : [51]

$$\lim_{h \rightarrow 0^\pm} \lim_{L \rightarrow \infty} M = \pm m_0, \quad m_0 = (1 - g^2)^{1/8}, \quad (6)$$

where  $M$  is the ground-state expectation value of the operator  $\hat{M} = L^{-1} \sum_x \hat{\sigma}_x^{(1)}$ .

In this paper, we present a numerical study of the zero-temperature phase diagram and the critical properties of the global model (1)-(2), based on extensive DMRG simulations [40] for systems with up to  $L = 65$  sites. Further details on the choice of the parameters for the numerical algorithm and on the accuracy of our simulations are provided in App. A. In our study we set  $J_e = J = 1$  without loss of generality (unless some specific limits are considered), and discuss quantum correlations within the ground state of the global model, in particular within  $\mathcal{S}$ , when varying the Hamiltonian parameters  $g, g_e$ , and  $w$ .

It is worth mentioning that other types of couplings between the two SQI chains can also be considered, which break, or partially break, the  $\mathbb{Z}_2 \oplus \mathbb{Z}_2$  symmetry of the decoupled quantum Ising systems. For example, one may consider the same Hamiltonian model (1), in which the local interaction term  $\hat{H}_w$  of Eq. (2c) is replaced by

$$\hat{H}_\kappa = -\kappa \sum_x \hat{\sigma}_x^{(1)} \hat{\tau}_x^{(1)}, \quad (7)$$

which breaks the  $\mathbb{Z}_2$  symmetries of the Ising chains, leaving a residual combined  $\mathbb{Z}_2$  symmetry when one simultaneously changes  $\hat{\sigma}_x^{(1)} \rightarrow -\hat{\sigma}_x^{(1)}$  and  $\hat{\tau}_x^{(1)} \rightarrow -\hat{\tau}_x^{(1)}$ . A study of the effects of the interaction  $\hat{H}_\kappa$  on SQI systems has been reported in Ref. [36]. As we shall see below, different scenarios emerge when the interaction between the stacked systems preserves the  $\mathbb{Z}_2$  symmetries of the subsystems, such as the one described by the Hamiltonian term  $\hat{H}_w$  in Eq. (2c).

## B. Observables

To study the equilibrium properties of the subsystem  $\mathcal{S}$  when the global system is in the ground state  $|\Psi_0\rangle$ , considering the other Ising chain as the environment  $\mathcal{E}$ , one may introduce its reduced density matrix

$$\hat{\rho}_{\mathcal{S}} = \text{Tr}_{\mathcal{E}} [|\Psi_0\rangle\langle\Psi_0|], \quad (8)$$

where  $\text{Tr}_{\mathcal{E}}[\cdot]$  denotes the partial trace over the Hilbert space associated with the subsystem  $\mathcal{E}$ .

Due to the global  $\mathbb{Z}_2$  symmetry, the expectation value of  $\hat{\sigma}_x^{(1)}$  vanishes, i.e.,  $\text{Tr}[\hat{\rho}_{\mathcal{S}} \hat{\sigma}_x^{(1)}] = 0$ . Therefore we consider its two-point correlation function

$$G(x, y) \equiv \text{Tr}[\hat{\rho}_{\mathcal{S}} \hat{\sigma}_x^{(1)} \hat{\sigma}_y^{(1)}]. \quad (9)$$

We recall that translation invariance is not preserved in systems with OBC, thus  $G(x, y)$  depends on both spatial positions  $x$  and  $y$ . Since we consider odd values of  $L = 2\ell + 1$ , and choose coordinates such that  $-\ell \leq x \leq \ell$ , we identify a central site,  $x_0 = 0$ .

In the following, we mostly focus on the correlations

$$G_0(x) \equiv G(x_0, x) \quad (10)$$

between the central point and the other sites. We also consider the susceptibility  $\chi_0$  and the second-moment correlation length  $\xi_0^2$  associated with the two-point function  $G_0(x)$ , defined as

$$\chi_0 = \sum_x G_0(x), \quad \xi_0^2 = \frac{1}{2\chi_0} \sum_x x^2 G_0(x). \quad (11)$$

Within the subsystem  $\mathcal{S}$ , one may also address the correlations of the transverse operators  $\hat{\sigma}_x^{(3)}$ , defined as

$$F(x, y) \equiv \text{Tr}[\hat{\rho}_{\mathcal{S}} \hat{\sigma}_x^{(3)} \hat{\sigma}_y^{(3)}] - \text{Tr}[\hat{\rho}_{\mathcal{S}} \hat{\sigma}_x^{(3)}] \text{Tr}[\hat{\rho}_{\mathcal{S}} \hat{\sigma}_y^{(3)}], \quad (12)$$

and the corresponding  $F_0(x) \equiv F(x_0, x)$ .

## III. SCALING BEHAVIORS FOR WEAKLY COUPLED ISING CHAINS

We now discuss the scaling behaviors of weakly interacting Ising chains, i.e., for small values of  $w$ , when the subsystem  $\mathcal{S}$  is close to criticality ( $g \approx g_{\mathcal{I}} = 1$ ). As shown in Ref. [36], when the intercoupling is driven by  $\hat{H}_\kappa$  [cf. Eq. (7)], the critical dependence on the coupling parameter  $\kappa$  strongly depends on the phase of the environment chain, i.e., whether its parameter  $g_e$  is larger, equal, or smaller than  $g_{\mathcal{I}}$ . Here, we instead study the critical scenarios emerging in  $\mathcal{S}$  when the interaction is driven by the symmetry-preserving Hamiltonian term  $\hat{H}_w$  of Eq. (2c). We anticipate that, while a crucial dependence on the environmental state persists, substantial differences arise compared to the scaling behavior found for the symmetry-breaking interaction  $\hat{H}_\kappa$ .

In this section we focus on situations in which the environment  $\mathcal{E}$  is far from criticality, meaning that  $g_e$  is sufficiently different from the Ising critical value  $g_e = g_{\mathcal{I}} = 1$ . The most interesting case, in which  $\mathcal{E}$  also presents critical correlations, will be discussed in Sec. IV.

### A. Ising transition lines

In the following we argue that, for both cases  $g_e > g_{\mathcal{I}}$  and  $g_e < g_{\mathcal{I}}$ , corresponding to a disordered or an ordered environment  $\mathcal{E}$ , a weak interaction  $\hat{H}_w$  only gives rise to a shift of the critical value of the Ising transition, from  $g = g_{\mathcal{I}}$  for  $w = 0$  to

$$g_c(w, g_e) \approx g_{\mathcal{I}} + c(g_e) w \quad (13)$$

for sufficiently small values of  $w$ , and the critical behavior of the correlation functions in  $\mathcal{S}$  remains within the 2D Ising universality class.

The behavior (13) can be derived using RG arguments. Since the environment chain is supposed to be noncritical and the expectation value of  $\hat{\tau}_x^{(3)}$  is nonzero for any value of  $g_e$  (see, e.g., Refs. [51, 52]), the effect of the intercoupling  $\hat{H}_w$  should effectively correspond to a further  $w$ -dependent term proportional to  $\hat{\sigma}_x^{(3)}$  in the Hamiltonian  $\hat{H}_{\mathcal{S}}$  associated with the subsystem  $\mathcal{S}$  [cf. Eq. (2a)]. Therefore, the quantum Ising transition of the isolated  $\mathcal{S}$  should only get shifted to a  $w$ -dependent critical value  $g_c(w, g_e)$ . In other words, the effect of a small coupling  $w$  can be effectively taken into account by adding an analytical dependence to the even scaling field  $u_r$  associated with the quantum Ising transition, i.e.,

$$u_r(g, w, g_e) \approx r - c(g_e) w, \quad r = g - g_{\mathcal{I}}, \quad (14)$$

where the nonuniversal constant  $c$  generally depends on the environment coupling  $g_e$  (we also fix an arbitrary normalization requiring  $u_r \approx r$  for  $w = 0$ ). Therefore the singular part of the free-energy density in the zero-temperature and FSS limit is expected to scale as [39, 53]

$$F_{\text{sing}}(g, w, L) \approx L^{-(d+z)} \mathcal{F}(u_r L^{y_r}), \quad (15)$$

where  $y_r = 1$  is the inverse length-scale critical exponent of the 2D Ising universality class. Since the critical point must correspond to the vanishing of the scaling field  $u_r$ , we obtain the linear relation (14) for the critical line at finite small values of  $w$  and for any fixed value of  $g_e$  far from the Ising critical value  $g_e \approx g_{\text{I}}$ .

## B. FSS along the Ising transition lines

To check the prediction (13) for the  $w$ -dependence of the transition lines and the 2D Ising universality class of the critical behaviors along these transition lines, we present a numerical analysis based on DMRG computations and their matching with the expected FSS behaviors at a quantum Ising transition [39, 53]. We focus on the correlation functions within the subsystem  $\mathcal{S}$  and study the effects of a small intercoupling with the environment  $\mathcal{E}$  (i.e., for small  $w$ ), when the Hamiltonian parameter of  $\mathcal{E}$  is far from the critical value  $g_{\text{I}}$  of the isolated subsystem. Namely, we consider  $g_e = 2$  and  $g_e = 0.5$ .

Assuming that the critical behaviors along the transition lines for small  $w$  belong to the 2D Ising universality class, the asymptotic FSS behavior of the two-point functions of the longitudinal and transverse spin operators [cf. Eqs. (9) and (12)], is expected to be given by [39, 53]

$$G(x_1, x_2) \approx L^{-2y_\phi} \mathcal{G}(X_1, X_2, u_r L^{y_r}), \quad (16)$$

$$F(x_1, x_2) \approx L^{-2y_e} \mathcal{F}(X_1, X_2, u_r L^{y_r}), \quad (17)$$

where

$$X_i = \frac{x_i}{2\ell}, \quad L = 2\ell + 1 \quad (18)$$

[for convenience we rescale distances using  $2\ell = L - 1$ , the difference in the asymptotic FSS limit only giving rise to  $O(L^{-1})$  corrections],  $u_r$  is the scaling field given in Eq. (14),  $y_\phi$  and  $y_e$  are the RG dimensions of the order-parameter field and energy operators, given respectively by  $y_\phi = (d + z - 2 + \eta)/2 = 1/8$  and  $y_e = d + z - y_r = 2 - y_r = 1$ . The scaling functions  $\mathcal{G}$  and  $\mathcal{F}$  are universal with respect to microscopic details of the model, but they depend on the boundary conditions. CFT allows us to determine them (see App. B for details).

The ratio between the correlation length  $\xi_0$ , cf. Eq. (11), and the size of the chain,

$$R_\xi = \xi_0/L, \quad (19)$$

is an RG invariant quantity. In the FSS limit, it scales as [39, 53]

$$R_\xi(g, w, L) = \mathcal{R}_\xi(u_r L^{y_r}) + O(L^{-\zeta}) + O(L^{-1}), \quad (20)$$

where  $u_r$  is given in Eq. (14),  $\mathcal{R}_\xi$  is a universal function apart from a rescaling of its argument, and the leading scaling corrections are controlled by the exponent  $\zeta =$

$2 - z - \eta = 3/4$ . In particular, at the critical point  $g = g_c$ , thus  $u_r = 0$ ,  $R_\xi$  behaves as [39, 53]

$$R_\xi(g_c, w, L) = R_\xi^* + a_\zeta L^{-\zeta} + a_1 L^{-1} + a_\omega L^{-\omega} + \dots \quad (21)$$

where  $R_\xi^* = \mathcal{R}_\xi(0)$  is an universal value which depends on the boundary conditions. For OBC, the critical value associated with the 2D Ising universality class is  $R_\xi^* \approx 0.159622$  (see App. B). There are various sources of power-law suppressed scaling corrections. The  $O(L^{-\zeta})$  scaling correction arises from the background analytical term of the susceptibility at the denominator of the second-moment correlation length [39, 53]. The  $O(L^{-1})$  correction is instead related to the boundary corrections associated with the OBC. Finally, the  $O(L^{-\omega})$  scaling correction with  $\omega = 2$  is related to the leading irrelevant RG perturbation at the 2D Ising fixed point [54, 55]. Note also that, since  $R_\xi$  is generally a monotonic function of  $u_r$ , the FSS behavior (20) implies that the curves of  $R_\xi$  for different lattice sizes  $L$  and  $L_2 > L$  cross each other, at a value of  $g$  that approaches  $g_c$  with  $O(L^{-1/\nu - \zeta})$  corrections, thus  $O(L^{-7/4})$  for Ising-like transitions, and the corresponding value of  $R_\xi$  approaches  $R_\xi^*$  with corrections that decay as  $L^{-\zeta}$ .

Other RG invariant quantities are obtained by taking the ratios of the correlation function  $G$  at different distances, such as

$$R_G(X_1, X_2) = \frac{G_0(x_1 = 2\ell X_1)}{G_0(x_2 = 2\ell X_2)}, \quad (22)$$

which are expected to scale similarly to  $R_\xi$ , i.e.,

$$R_G(X_1, X_2, g, w, L) = \mathcal{R}_G(X_1, X_2, u_r L^{y_r}) + O(L^{-1}) \quad (23)$$

where  $\mathcal{R}_G$  is a function that is universal apart from a rescaling of its argument  $u_r L^{y_r}$  [53, 54]. In particular, at the critical point,  $R_\xi$  behaves as [53]

$$R_G(X_1, X_2) = R_G(X_1, X_2)^* + O(L^{-1}). \quad (24)$$

Using CFT, one can compute  $R_G(X_1, X_2)^*$ , for example  $R_G^*(1/8, 1/4) \approx 1.358609$  (see App. B). In the above formulas for  $R_G$ , the leading scaling corrections are expected to arise from the boundaries, thus they are  $O(L^{-1})$  for OBC. Note that the ratios  $R_G$ , unlike  $R_\xi$ , are not affected by the analytical  $O(L^{-\zeta})$  contributions at the critical point.

## C. Numerical results

We now present a numerical analysis for  $g_e = 2$  and  $g_e = 0.5$ , at small values of  $w$ , for values of  $g$  around  $g_{\text{I}} = 1$ . As we shall see, the results nicely match the FSS behaviors discussed above, confirming that the critical behavior of the transition lines originating from  $g = 1$  and  $w = 0$  remains Ising-like.

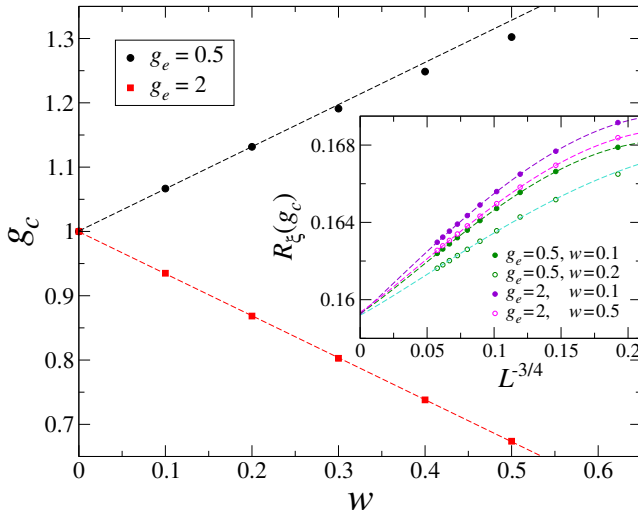


FIG. 2: The critical value  $g_c$  of the Ising transition as a function of  $w$  for a model of weakly coupled Ising chains, described by the Hamiltonian (1)-(2). The two data sets are for  $g_e = 0.5$ , black dots, and  $g_e = 2$ , red squares (the uncertainty on the estimates of  $g_c$  are smaller than the symbols). The dashed lines show linear fits of the critical points for  $w \lesssim 0.2$  to  $g_c(w, g_e) = g_{\mathcal{I}} + c(g_e)w$ , which is the expected behavior for sufficiently small values of  $w$  (see text). The inset shows  $R_{\xi}$  vs  $L^{-3/4}$  at the crossing point between data for sizes  $L$  and  $L+4$ , at fixed  $g_e$  and  $w$  (symbols correspond to sizes ranging from  $L = 9$  to  $L = 45$ , in increments of four). Dashed curves are fits to the corresponding numerical data, for  $L \geq 13$ , according to the predicted behavior (21).

The  $w$ -dependence of the critical points  $g_c(w, g_e)$  can be straightforwardly obtained by matching our data (we performed simulations up to  $L = 49$ ) for the RG invariant quantities  $R_{\xi}$  and  $R_G(X_1, X_2)$  at fixed small  $w$  with their expected FSS behavior at Ising-like transitions [see Eqs. (20) and (23)]. In particular, the values at the crossing points of  $R_{\xi}$  and  $R_G(1/8, 1/4)$  for different sizes appear to converge to the corresponding universal values of the 2D Ising universality class, namely  $R_{\xi}^* = 0.159622$  and  $R_G^*(1/8, 1/4) = 1.358609$  (see App. B). For example, the inset of Fig. 2 shows the crossing points of  $R_{\xi}$  for sizes  $L$  and  $L+4$  plotted versus  $L^{-3/4}$ , corresponding to the expected leading power-law scaling corrections. They appear to converge to the Ising value with an accuracy of about  $5 \times 10^{-4}$ . These results confirm that the transitions belong to the 2D Ising universality class.

The critical points  $g_c(w, g_e)$  can be then straightforwardly obtained by fitting the  $R_{\xi}$  data to the FSS ansatz (20), using the Ising values  $R_{\xi}^* = 0.159622$  and  $\nu = 1$ , and also including the expected  $O(L^{-3/4})$  scaling corrections. Close to  $g_c$ , low-order polynomial approximations of the scaling function  $\mathcal{R}_{\xi}(u_r L^{1/\nu})$  are sufficient. Analogous results are obtained by analyzing the data of the ratios  $R_G(X_1, X_2)$ . This procedure allows us to obtain accurately estimates of  $g_c(w, g_e)$ , as shown in Fig. 2. These results are in good agreement with the linear  $w$ -

dependence predicted by the RG arguments reported in Sec. III A [cf. Eq. (13)]. Note, however, that deviations from the expected behavior emerge at smaller values of  $w$  for  $g_e = 0.5$  than for  $g_e = 2$ .

We finally remark that the scaling behavior of the subsystem  $\mathcal{S}$  appears to be the same, when the Hamiltonian parameter  $g_e$  of the environment  $\mathcal{E}$  corresponds to either the paramagnetic ( $g_e > 1$ ) or the ferromagnetic ( $g_e < 1$ ) phase. This behavior is markedly different from that observed when the interactions between the SQI subsystems are driven by the Hamiltonian term (7), which breaks the global symmetry of the decoupled subsystems. In that case, the scaling behaviors turn out to substantially differ between  $g_e > 1$  and  $g_e < 1$  [36]. As we shall see, the scenario becomes more complex when both subsystems are critical, i.e., when  $g \approx g_e \approx g_{\mathcal{I}}$ .

#### IV. SCALING BEHAVIORS IN THE LIMIT OF EQUAL SUBSYSTEMS

We now concentrate on the scenario in which the SQI chains are critical, with both couplings  $g$  and  $g_e$  close to the critical value  $g_{\mathcal{I}} = 1$ . To simplify our analysis, we consider the symmetric case  $g = g_e$ , corresponding to the 1D QAT model described by Hamiltonian (1)-(2) with  $J = J_e = 1$  and  $g = g_e$ . The QAT model is symmetric under the independent  $\mathbb{Z}_2$  parity symmetries:  $\hat{\sigma}_x^{(1,2)} \rightarrow -\hat{\sigma}_x^{(1,2)}$  keeping  $\hat{\sigma}_x^{(3)}$  unchanged,  $\hat{\tau}_x^{(1,2)} \rightarrow -\hat{\tau}_x^{(1,2)}$  keeping  $\hat{\tau}_x^{(3)}$  unchanged, and the  $\mathbb{Z}_2$  interchange symmetry  $\hat{\sigma}_x \leftrightarrow \hat{\tau}_x$ . In particular, for  $w = 0$ , two identical and decoupled quantum Ising chains are recovered.

Some studies related to the 1D QAT model have been reported in Refs. [41–47, 56–64]. In the following, we focus on the FSS behavior of the 1D QAT model along its continuous quantum transition line where the length-scale critical exponent  $\nu$  varies continuously.

##### A. The critical line of the QAT chain

The phase diagram of the 1D QAT model shows a peculiar line of continuous transitions with central charge  $c = 1$ , where the length-scale critical exponent changes continuously, along the line  $g = g_c = 1$  and  $-1/\sqrt{2} \leq w \leq 1$ . Along this transition line,  $w$  represents a marginal parameter, i.e., its RG dimension vanishes at the corresponding line of fixed points. At fixed  $w$ , when varying  $g$  around  $g_c$ , the divergence of the length scale of the critical modes is controlled by a continuously varying critical exponent  $\nu$ , whose dependence on the Hamiltonian parameter  $w$  has been predicted to be [41, 47]

$$\nu(w) = \frac{2 \arccos(-w)}{4 \arccos(-w) - \pi}, \quad (25)$$

on the basis of a mapping to the exactly solvable six-vertex model [65, 66]. Therefore, along the transition

line, the length-scale exponent varies from  $\nu = 2/3$  for  $w = 1$  (corresponding to the  $q = 4$  Potts model) to  $\nu \rightarrow \infty$  for  $w \rightarrow -1/\sqrt{2}$  (for example we have  $\nu = 4/5$  for  $w = 1/2$ ,  $\nu = 1$  for  $w = 0$ , and  $\nu = 2$  for  $w = -1/2$ ). On the other hand, the critical exponent  $\eta = 1/4$  (associated with the RG dimension  $y_\phi = \eta/2$  of the order-parameter field) and the dynamic exponent  $z = 1$  (associated with the power-law suppression of the gap at the critical point) remain the same along the line.

This peculiar behavior of the critical exponents, and in particular the dependence of  $\nu$  on  $w$ , have been confirmed by various numerical analyses (see, e.g., Refs. [47, 60–62]), with a reasonable accuracy (the most recent Refs. [61, 62] mention that their estimates of  $\nu$  have a relative accuracy of 5–10% sufficiently far from the boundaries  $w = -1/\sqrt{2}$  and  $w = 1$  of the interval where continuous transitions occur). We have checked the formula (25) by FSS analyses of our DMRG data at fixed  $w$  and around  $g_c = 1$ . For this purpose, the optimal observables are provided by the RG invariant ratios  $R_G(X_1, X_2)$ , defined in Eq. (22), whose scaling behavior at fixed  $w$  is expected to be

$$R_G(X_1, X_2, g, w, L) \approx \mathcal{R}_G[X_1, X_2, (g - g_c)L^{1/\nu}]. \quad (26)$$

The ratios  $R_G$  are expected to yield more precise results than  $R_\xi$  [cf. Eq. (19)], because their FSS is not affected by analytic corrections (see the discussion in Sec. III B).

A straightforward analysis of our DMRG data for  $R_G(1/8, 1/4)$  at fixed  $w = -0.5$  and  $w = +0.5$ , up to  $L = 65$ , by matching them to the asymptotic scaling Eq. (26), and in particular to its linear approximation  $R_G^*(1/8, 1/4) + a(g - g_c)L^{1/\nu}$ , leads to precise estimates  $R_G(1/8, 1/4) = 1.2456(1)$  and  $\nu = 2.02(2)$  for  $w = -0.5$ , and  $R_G(1/8, 1/4) = 1.491(1)$  and  $\nu = 0.802(8)$  for  $w = +0.5$ , with a relative accuracy of about 1% (these results can be compared with the Ising values  $R_G(1/8, 1/4) = 1.358609$  and  $\nu = 1$ ). These findings are obtained from fits of the largest lattices in the range  $33 \lesssim L \leq 65$ ; the errors take into account the variation of the fitted values, when changing the minimum system size included in the fit and the linear fitting ansatzes using  $L$  or  $2\ell$ , thus somehow quantifying the effects of the  $O(L^{-1})$  scaling corrections. The outcomes are in excellent agreement with the exact results from Eq. (25) (i.e.,  $\nu = 2$  for  $w = -0.5$ , and  $\nu = 0.8$  for  $w = 0.5$ ). We do not report further details, as they are not particularly illuminating for the purposes of this paper. In the following, we assume the validity of the formula in Eq. (25) for the values of the critical exponent  $\nu$ .

The phase diagram for values of  $w$  outside the range  $w \in [-1/\sqrt{2}, 1]$  presents other transition lines, where quantum critical behaviors are expected to belong to the 2D Ising and Berezinskii-Kosterlitz-Thouless universality classes [41, 42, 46, 59]. In particular, the extremal critical point  $g = 1$ ,  $w = 1$ , corresponding to a quantum  $q = 4$  state Potts model, is the starting point of two Ising transition lines for  $w > 1$  and  $g \neq 1$ . We also note that a number of studies of the phase diagram and critical behavior

of the 2D CAT model are reported in Refs. [49, 67–76]. In the following, we focus on the most peculiar transition line of the QAT chain where the critical exponent  $\nu$  changes, thus for  $g \approx 1$  and  $w \in [-1/\sqrt{2}, 1]$ , which contains the weak intercoupling regime. We will not discuss the other more standard transition lines of the phase diagram for  $w < -1/\sqrt{2}$  and  $w > 1$ .

## B. FSS of the correlation functions within $\mathcal{S}$

To study the critical behavior within  $\mathcal{S}$ , we focus on the correlation functions of the longitudinal  $\hat{\sigma}_x^{(1)}$  and transverse  $\hat{\sigma}_x^{(3)}$  spin operators, defined in Eqs. (9) and (12), respectively. Note that they are equal to the analogous correlation functions of the operator  $\hat{\tau}_x^{(1)}$  and  $\hat{\tau}_x^{(3)}$ , because of the  $\mathbb{Z}_2$  interchange symmetry  $\hat{\sigma}_x \leftrightarrow \hat{\tau}_x$  of the QAT model.

### 1. The longitudinal correlation function

Since  $w$  is a marginal parameter along the continuous transition line, due to the fact that its RG dimension vanishes, the two-point function along the critical line, i.e., varying  $w$  within  $[-1/\sqrt{2}, 1]$  and keeping  $g = 1$  fixed, is expected to show the FSS behavior

$$G(x_1, x_2; w) \approx L^{-2y_\phi} \mathcal{G}(X_1, X_2; w), \quad (27)$$

where  $X_i \approx x_i/L$  and  $y_\phi = \eta/2 = 1/8$  is the  $w$ -independent RG dimension of the order-parameter field corresponding to  $\hat{\sigma}_x^{(1)}$  and  $\hat{\tau}_x^{(1)}$ . In the case of boundary conditions preserving translational invariance, such as PBC,  $G(x_1, x_2) \equiv G(x_2 - x_1)$ . We recall that the scaling function  $\mathcal{G}$  is expected to depend on the boundary conditions. An interesting question concerns its dependence on  $w$  (i.e., whether, and how, it depends on  $w$ ).

Some exact results for the scaling behavior of the critical two-point function can be obtained by CFT approaches (see, e.g., Refs. [77, 78]). Interestingly, in the case of PBC preserving translational invariance, no differences are expected in the FSS of the two-point function  $G(x - y) = \text{Tr}[\hat{\rho}_{\mathcal{S}} \hat{\sigma}_x^{(1)} \hat{\sigma}_y^{(1)}]$  along the continuous transition line. Indeed, conformal invariance strongly constrains its behavior when considering PBC, leading to the simple behavior

$$G_{\text{pbc}}(x) \propto [L^2 \sin^2(\pi X)]^{-y_\phi}. \quad (28)$$

Therefore, its critical FSS function

$$\mathcal{G}_{\text{pbc}}(X) = [\sin(\pi X)]^{-2y_\phi} \quad (29)$$

depends only on the RG dimension  $y_\phi = 1/8$  of the order parameter field (the overall constant is related to an irrelevant normalization)—see, e.g., Refs. [77, 78]. Since the RG dimension  $y_\phi$  remains the same along the continuous transition line, the FSS of the two-point function for

PBC, and its related quantities turns out to be independent of  $w$ , i.e., it does not change along the continuous transition line for  $-1/\sqrt{2} < w \leq 1$ .

This behavior of the two-point function with PBC may suggest that the FSS along the continuous transition line remains unchanged. In this respect we mention that the numerical analyses of Ref. [73] did not observe variations of the FSS of the 2D CAT model with PBC along the transition line where the exponent  $\nu$  varies continuously, putting forward a *superuniversality* hypothesis [73, 79], that is that the scaling functions remain unchanged along the fixed-point line of the CAT model (up to trivial normalizations). In the following we show that this simple scenario is not confirmed by our FSS analysis of the QAT model with OBC. We recall that, using the quantum-to-classical mapping, the FSS of the 1D QAT model is expected to be analogous to that of the 2D CAT model within an infinite slab, with the same boundary conditions along the finite-size direction [38, 39].

For OBC, which does not preserve translational invariance, it is more convenient to rescale the coordinate as  $X = x/(L-1)$ , especially when using odd sizes  $L = 2\ell+1$ , and consider the correlation functions

$$G_0(x) \equiv G(x_0, x) \approx L^{-2y_\phi} G_0(X), \quad X = \frac{x}{2\ell}, \quad (30)$$

where  $x_0 = 0$  is the central site of the chain, and  $X \in [-1/2, 1/2]$ . The FSS of the two-point correlation function  $G_0(x)$  with OBC turns out to be more complex than that with PBC, due to the presence of the boundaries. Therefore a numerical analysis of  $G_0(x)$  for OBC should provide a nontrivial check of the  $w$ -dependence of the critical behaviors along the QAT transition line. Its exact behavior is known for the critical Ising chain, showing a more complex structure (see App. B).

In Fig. 3 we show results for the two-point longitudinal correlator function, for various values of  $w$ , as obtained by DMRG computations up to  $L = 65$ , and compare them with the exact CFT expressions for the quantum Ising chain ( $w = 0$ ), see App. B. For an optimal comparison of the scaling behaviors for different values of  $w$ , we plot the ratios  $R_G(X_1, X_2 = 1/8)$  defined in Eq. (22), which allows us to eliminate the nonuniversal multiplicative normalization of the critical two-point function. For these quantities, the asymptotic FSS behavior is expected to be given

$$R_G(X_1, X_2; w) = R_G^*(X_1, X_2; w) + a_1 L^{-1} + a_\omega L^{-\omega} + \dots \quad (31)$$

where the  $O(L^{-1})$  term is related to the boundary corrections associated with the OBC, and the  $O(L^{-\omega})$  scaling correction is related to the leading irrelevant RG perturbation at the fixed point, which may depend on  $w$ . We recall that  $\omega = 2$  for the Ising chain [54, 55]. The results for the ratios  $R_G(X_1, X_2 = 1/8; w)$  reported in Fig. 3 clearly show that they approach an asymptotic FSS, as predicted by Eq. (31), and their large- $L$  behavior appears to be well described by  $O(L^{-1})$  corrections (see the inset of Fig. 3), suggesting that  $\omega \gtrsim 1$  for all values of  $w$ .

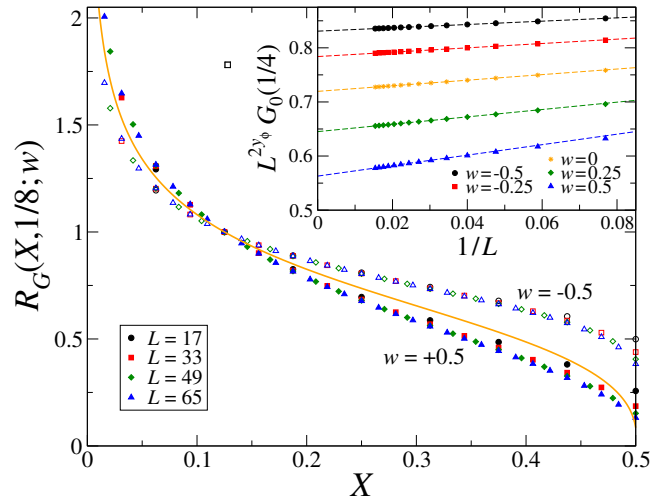


FIG. 3: The scaling behavior of the ratio  $R_G(x_1 = 2\ell X, x_2 = \ell/4)$ , defined in Eq. (22). We report data for  $w = -0.5$  (empty symbols) and  $0.5$  (full symbols), up to  $L = 65$ . They confirm the approach to asymptotic  $w$ -dependent FSS curves, as predicted by Eq. (31). The full line shows the exact result for the critical quantum Ising chain ( $w = 0$ ), obtained by the CFT approach (see App. B). The inset shows results for  $G_0(\ell/4)$  vs  $1/L$ , for various values of  $w$ , confirming its asymptotic  $L^{-2y_\phi}$  power-law scaling with  $1/L$  corrections (dashed lines are linear fits to the numerical data for  $L \geq 25$ ).

considered. Moreover, they definitely show that the FSS of the two-point function with OBC depends on  $w$ , at variance with the case of PBC where the FSS (29) of the two-point function is independent of  $w$ .

## 2. The transverse correlation function

One may also study the scaling behavior of the two-point function of the transverse spin operator  $\hat{\sigma}_x^{(3)}$ , defined in Eq. (12). We expect that its FSS behavior along the QAT transition line  $g = 1$  and  $w \in [-1/\sqrt{2}, 1]$  can be written as

$$F(x_1, x_2; w) \approx L^{-\kappa} \mathcal{F}(X_1, X_2; w), \quad (32)$$

with an appropriate exponent  $\kappa$  that should be related to some of the RG operators at the QAT fixed points. We recall that, at a standard Ising transition (i.e., when the stacked subsystems are decoupled), the scaling behavior is the one reported in Eq. (17), with  $\kappa = 2y_e$  where  $y_e = d + z - y_r = 1$ , due to the fact that the transverse operator  $\hat{\sigma}_x^{(3)}$  is related to the energy-density operator at the 2D Ising fixed point.

To check the scaling of the  $\hat{\sigma}_x^{(3)}$  correlations, we also define the correlations  $F_0(x) = F(x_0, x)$  with the central point of the lattice, and the ratios

$$R_F(X_1, X_2) = \frac{F_0(x_1 = 2\ell X_1)}{F_0(x_2 = 2\ell X_2)}. \quad (33)$$

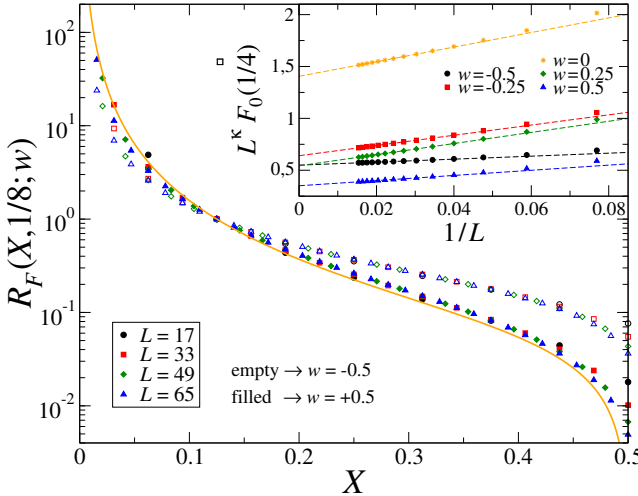


FIG. 4: The scaling behavior of the ratio  $R_F(X, 1/8)$ , defined in Eq. (33), for  $w = -0.5$  and  $0.5$ . They confirm the approach to asymptotic  $w$ -dependent FSS curves, as predicted by Eq. (32). The full line shows the exact result for the critical quantum Ising chain ( $w = 0$ )—see App. B. The inset shows results for  $F_0(\ell/4)$  vs  $1/L$ , confirming its asymptotic  $L^{-\kappa}$  power-law scaling with  $1/L$  corrections, with  $\kappa$  given by Eq. (38) (dashed lines are linear fits to the numerical data for  $L \geq 25$ ).

Our numerical analysis confirms the scaling behavior reported in Eq. (32), as demonstrated by the data for the ratio  $R_F(X, 1/8)$  shown in Fig. 4, which appear to approach asymptotic  $w$ -dependent scaling curves. However, this check does not provide information on the value of  $\kappa$  itself. The determination of the exponent  $\kappa$  in the QAT correlation function  $F(x, y)$  turns out to be more complicated than that at the quantum Ising transitions, because there are two independent RG operators associated with  $\hat{\sigma}_x^{(3)}$ . Indeed, we may write

$$\hat{\sigma}_x^{(3)} = \hat{E}_x + \hat{C}_x, \quad (34)$$

$$\hat{E}_x = \hat{\sigma}_x^{(3)} + \hat{\tau}_x^{(3)}, \quad \hat{C}_x = \hat{\sigma}_x^{(3)} - \hat{\tau}_x^{(3)}, \quad (35)$$

where  $\hat{E}_x$  and  $\hat{C}_x$  are operators associated with different RG perturbations [41, 68, 80] of the  $w$ -dependent fixed points along the QAT transition line. The operator  $\hat{E}_x$  can be associated with the energy RG perturbation controlling the critical behavior when changing  $g$ , thus

$$y_e = d + z - \frac{1}{\nu} = \frac{2\nu - 1}{\nu}, \quad (36)$$

with the  $w$ -dependent exponent  $\nu$  reported in Eq. (25). The other operator  $\hat{C}_x$ , called crossover operator [41], has a different RG dimension given by [41, 80]

$$y_c = y_e^{-1} = \frac{\nu}{2\nu - 1}. \quad (37)$$

The asymptotic FSS behavior of the  $\hat{\sigma}_x^{(3)}$  correlation function (32) must be controlled by the smallest RG dimension between  $y_e$  and  $y_c$ , therefore the exponent  $\kappa$  in

Eq. (32) should be given by <sup>1</sup>

$$\kappa = 2 \text{Min}[y_e, y_c]. \quad (38)$$

Notice that  $y_e = y_c$  when  $\nu = 1$ , which corresponds to the case of the Ising universality class, thus for  $w = 0$ . Therefore, we have  $\kappa = 2y_e$  for  $w > 0$  and  $\kappa = 2y_c$  for  $w < 0$ . For example, this would imply that  $\kappa = 3/2$  for  $w = 0.5$  and  $\kappa = 4/3$  for  $w = -0.5$ . The formula for  $\kappa$  reported in Eq. (38) is nicely confirmed by our numerical simulations, see, for example, the inset of Fig. 4, which shows data for the correlation  $F(0, \ell/4)$  for various values of  $w$ .

### 3. Other correlation functions

We have also computed the FSS behavior of correlation functions involving the spin operator of the environment  $\mathcal{E}$ . In particular, we verified the FSS of the connected correlation function of the energy operator  $\hat{E}_x$  defined in Eq. (35),

$$E(x_1, x_2) = \langle \Psi_0 | \hat{E}_{x_1} \hat{E}_{x_2} | \Psi_0 \rangle - \langle \Psi_0 | \hat{E}_{x_1} | \Psi_0 \rangle \langle \Psi_0 | \hat{E}_{x_2} | \Psi_0 \rangle, \quad (39)$$

where  $|\Psi_0\rangle$  is the ground state of the QAT model. Numerical data (not shown) nicely support the expected asymptotic FSS behavior

$$E(x_1, x_2; w) \approx L^{-2y_e} \mathcal{E}(X_1, X_2; w), \quad (40)$$

with  $y_e$  given in Eq. (36). Note that this scaling behavior holds even for negative values of  $w$ , unlike the case of the transverse correlation function of the operator  $\hat{\sigma}_x^{(3)}$  [see Eq. (32) with  $\kappa$  given in Eq. (38)].

We finally consider the correlation function of the polarization operator  $\hat{P}_x = \hat{\sigma}_x^{(1)} \hat{\tau}_x^{(1)}$ , i.e.,

$$P(x_1, x_2) = \langle \Psi_0 | \hat{P}_{x_1} \hat{P}_{x_2} | \Psi_0 \rangle. \quad (41)$$

Its FSS behavior is expected to be

$$P(x_1, x_2; w) = L^{-2y_p} \mathcal{P}(X_1, X_2; w), \quad (42)$$

$$y_p = \frac{y_e}{4} = \frac{1}{2} - \frac{1}{4\nu}, \quad (43)$$

where  $y_p$  is the RG dimension of the operator  $\hat{P}_x$  [41, 49, 67, 68, 73], which depends on  $w$  as well (for example,  $y_p = 3/8$  for  $w = -1/2$  and  $y_p = 3/16$  for  $w = 1/2$ ). Note that, for  $w = 0$  (i.e., when the stacked Ising subsystems get decoupled), the correlation function  $P$  equals the square of the Ising-chain two-point function of the

<sup>1</sup> This can be understood by recalling that the critical spatial correlations of a generic operator  $\hat{O}(x)$  decay as  $G_O(x, y) \sim |x - y|^{-2y_o}$ . Therefore the correlations of operators with smaller RG dimensions  $y_o$  are less suppressed in the large-distance limit.

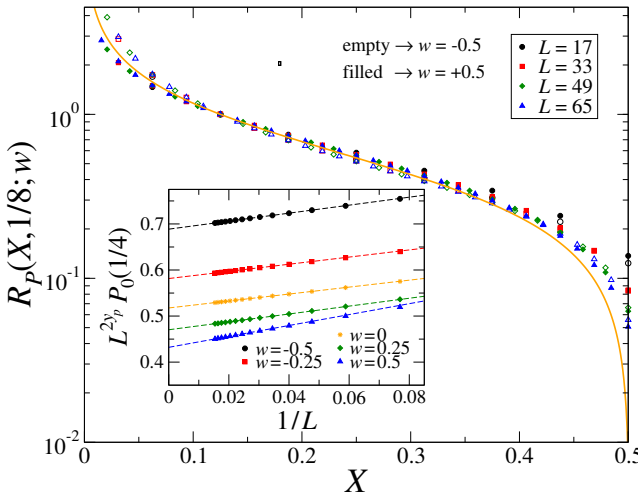


FIG. 5: The scaling behavior of the ratio  $R_P(X, 1/8)$ , defined in Eq. (44), for  $w = -0.5$  and  $0.5$ . They confirm the approach to asymptotic  $w$ -dependent FSS curves, as predicted by Eq. (42). The full line shows the exact result for the critical quantum Ising chain ( $w = 0$ )—see App. B. The inset shows results for  $P_0(\ell/4)$  vs  $1/L$ , confirming its asymptotic  $L^{-2y_p}$  power-law scaling with  $1/L$  corrections (dashed lines are linear fits to the numerical data for  $L \geq 25$ ).

longitudinal spin operator  $\hat{\sigma}_x^{(1)}$ . Therefore, we must have  $y_p = 2y_\phi = 1/4$  for  $w = 0$ , which is consistent with the value obtained by inserting the Ising value  $\nu = 1$  into Eq. (43). Analogously to the other correlation functions, we define the correlations  $P_0(x) = P(x_0, x)$  with the central point of the lattice, and the ratios

$$R_P(X_1, X_2) = \frac{P_0(x_1 = 2\ell X_1)}{P_0(x_2 = 2\ell X_2)}. \quad (44)$$

As shown in Fig. 5, the FSS behavior (42) of the  $P$ -correlation is nicely confirmed by the data.

### C. FSS of the ground-state fidelity

We finally discuss the FSS behavior of the ground-state fidelity when changing the Hamiltonian parameters along the fixed-point line of the QAT model. In fact, the quantum fidelity is able to provide information of the quantum critical correlations developed by the system [39, 81–83]. It is a geometrical object that can be used to monitor the changes in the ground-state wave function  $|\Psi_0(u, L)\rangle$  when one of the control parameters, say  $u$ , is varied by a small amount  $\varepsilon$ . The ground-state fidelity associated with a generic Hamiltonian parameter  $u$  is defined as

$$A(u, \varepsilon, L) \equiv |\langle \Psi_0(u + \varepsilon, L) | \Psi_0(u, L) \rangle|. \quad (45)$$

Of course,  $A(u, 0, L) = 1$ . Assuming  $\varepsilon$  to be sufficiently small, one can expand Eq. (45) in powers of  $\varepsilon$  [82]:

$$A(u, \varepsilon, L) = 1 - \frac{1}{2} \varepsilon^2 \chi_A(u, L) + O(\varepsilon^3), \quad (46)$$

where  $\chi_A$  defines the fidelity susceptibility (the cancellation of the linear term of the expansion is essentially related to the fact that the fidelity is bounded, i.e.,  $F \leq 1$ ). Under normal conditions, the fidelity susceptibility is expected to grow proportionally to the volume, i.e.,  $\chi_A \sim L^d$ . However, its power law can change drastically across a continuous transition driven by the Hamiltonian parameter  $u$  with RG dimension  $y_u$ . Indeed, one expects the behavior [39, 84]

$$\chi_A(u, L) \approx L^{2y_u} \mathcal{A}_2(u L^{y_u}). \quad (47)$$

Note, however, that Eq. (47) describes the leading scaling behavior only when  $2y_u > d$ . Otherwise, for  $2y_u < d$ , the power-law with increasing size is dominated by the analytic contributions at the continuous transition [39], i.e.,  $\chi_A \sim L^d$ , while the scaling term in Eq. (47) provides only a subleading contribution.

We may define an analogous ground-state fidelity susceptibility  $\chi_A(w, L)$  along the critical line of QAT model (thus for  $g = 1$ ), with respect to variations of the interaction parameter  $w$ . Since  $w$  is marginal along the critical line, meaning that its RG dimension  $y_w$  vanishes, we would expect the normal asymptotic large-size behavior

$$\chi_A(w, L) \sim L. \quad (48)$$

On the other hand, keeping  $w$  fixed and varying  $g$  around its critical value  $g = g_c = 1$ , whose RG dimension is  $y_g = 1/\nu$ , we expect the asymptotic large-size behavior

$$\chi_A(g, L) \approx L^{2/\nu} \mathcal{A}_2[(g - g_c)L^{1/\nu}] \quad \text{for } \nu < 2, \quad (49)$$

therefore for  $-1/2 < w \leq 1$ . On the other hand,  $\chi_A(g, L) \sim L$  for  $\nu \geq 2$ , corresponding to  $-1/\sqrt{2} < w \leq -1/2$ .

## V. TWO-DIMENSIONAL STACKED QUANTUM ISING SYSTEMS

In this section, we extend the discussion to higher-dimensional SQI models, in particular focusing on 2D SQI systems, while still assuming local interactions that preserve the  $\mathbb{Z}_2$  symmetry of each quantum Ising subsystem. These systems are defined analogously to the SQI chains, by extending the Hamiltonian terms (2) to higher dimensions, i.e.,

$$\hat{H}_\sigma = -J \sum_{\langle \mathbf{x} \mathbf{y} \rangle} \hat{\sigma}_\mathbf{x}^{(1)} \hat{\sigma}_\mathbf{y}^{(1)} - g \sum_{\mathbf{x}} \hat{\sigma}_\mathbf{x}^{(3)}, \quad (50a)$$

$$\hat{H}_\tau = -J_e \sum_{\langle \mathbf{x} \mathbf{y} \rangle} \hat{\tau}_\mathbf{x}^{(1)} \hat{\tau}_\mathbf{y}^{(1)} - g_e \sum_{\mathbf{x}} \hat{\tau}_\mathbf{x}^{(3)}, \quad (50b)$$

$$\hat{H}_w = -w \left[ \sum_{\langle \mathbf{x} \mathbf{y} \rangle} \hat{\sigma}_\mathbf{x}^{(1)} \hat{\sigma}_\mathbf{y}^{(1)} \hat{\tau}_\mathbf{x}^{(1)} \hat{\tau}_\mathbf{y}^{(1)} + \sum_{\mathbf{x}} \hat{\sigma}_\mathbf{x}^{(3)} \hat{\tau}_\mathbf{x}^{(3)} \right], \quad (50c)$$

where  $\hat{\sigma}_\mathbf{x}^{(k)}$  and  $\hat{\tau}_\mathbf{x}^{(k)}$  are two sets of Pauli matrices ( $k = 1, 2, 3$ ) on the site  $\mathbf{x}$ ,  $\langle \mathbf{x} \mathbf{y} \rangle$  denotes nearest-neighbor sites. As before, we consider  $J = J_e = 1$ .

Again, for  $w = 0$ , we have two decoupled quantum Ising systems. We recall that quantum Ising models in  $d \geq 2$  dimensions undergo a continuous transition as well, at a finite value  $g_c$ , belonging to the  $(d+1)$ -dimensional Ising universality class. Accurate estimates of the critical exponents of the 3D Ising universality class have been obtained using various approaches (see, e.g., Refs. [54, 85–91]); in particular [88],  $\nu = 0.629971(4)$ . The critical exponents of the 4D Ising universality class take mean-field values,  $\nu = 1/2$  and  $\eta = 0$ , with additional multiplicative logarithmic corrections [54]. The dynamic exponent  $z$  is 1 in any dimension.

The scenario in which the subsystem  $\mathcal{S}$  is close to criticality and weakly coupled to an environment  $\mathcal{E}$  far from criticality is analogous to that discussed in Sec. III, with transition lines belonging to the  $(d+1)$ -dimensional Ising universality class. Therefore, we focus on the case where both SQI subsystems are critical, leading to a distinct multicritical scenario in which an effective enlargement of the symmetry from  $\mathbb{Z}_2 \oplus \mathbb{Z}_2$  to  $O(2)$  takes place, thus differing substantially from that found for SQI chains.

In these conditions, the systems exhibit multicritical behaviors characterized by two relevant RG perturbations, both invariant under the global symmetry of the model and both of which must be tuned to reach the multicritical point. We indicate with  $r_1$  and  $r_2$  the corresponding parameters, normalized such that  $r_1 = r_2 = 0$  at the multicritical point. Of course, they must be functions of the SQI Hamiltonian parameters  $g$ ,  $g_e$ , and  $w$ . Assuming, reasonably, that the dynamic exponent at the multicritical point is  $z = 1$ , the competition between the order parameters of  $d$ -dimensional SQI models can be described by an effective  $(d+1)$ -dimensional Landau-Ginzburg-Wilson (LGW)  $\Phi^4$  theory. This theory involves two real order-parameter fields,  $\varphi_1$  and  $\varphi_2$ , which are invariant under a  $\mathbb{Z}_2 \oplus \mathbb{Z}_2$  symmetry, i.e., under the sign change of each field, so that only even powers of each field are allowed. The corresponding Hamiltonian is [92–94]

$$\mathcal{H} = (\partial_\mu \varphi_1)^2 + (\partial_\mu \varphi_2)^2 + r_1 \varphi_1^2 + r_2 \varphi_2^2 + v_1 \varphi_1^4 + v_2 \varphi_2^4 + v_3 \varphi_1^2 \varphi_2^2. \quad (51)$$

Mean-field analyses show that this theory admits a bicritical point [92–94], as sketched in Fig. 6. The 3D RG flow of the quartic couplings determines the 3D multicritical behavior when tuning the quadratic parameters  $r_1$  and  $r_2$  to the multicritical point. The stable fixed point of the  $\mathbb{Z}_2 \oplus \mathbb{Z}_2$  multicritical LGW theory (51) turns out to be the  $O(2)$ -symmetric XY fixed point [94–97]. Therefore, the multicritical behavior at the bicritical point of 2D  $\mathbb{Z}_2 \oplus \mathbb{Z}_2$  symmetric quantum systems must generally belong to the XY universality class,<sup>2</sup> thus realizing an ef-

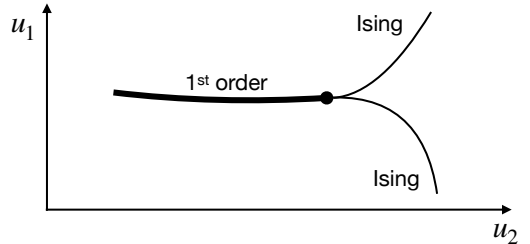


FIG. 6: Sketch of a phase diagram containing a 3D bicritical XY point arising from the competition of two distinct Ising-like order parameters, for generic system parameters  $u_1$  and  $u_2$ . The multicritical behavior at the bicritical XY point is described by the 3D LGW theory (51). It is located at the meeting point of three transition lines, one first-order transition line (thick full line) and two continuous Ising transition lines (full lines) whose order parameters are related to the real scalar fields  $\varphi_1$  and  $\varphi_2$  of the LGW theory (51). At the bicritical XY point the symmetry of the critical modes gets effectively enlarged, from  $\mathbb{Z}_2 \oplus \mathbb{Z}_2$  to  $O(2)$ .

fective enlargement of the symmetry of the multicritical modes, from  $\mathbb{Z}_2 \oplus \mathbb{Z}_2$  to  $O(2)$ .

For values of the QAT parameter  $w$  that are within the attraction domain of the bicritical XY point  $g = g_e = g_{mc}$  (where  $g_{mc}$  generally depends on  $w$ ), the singular part of the free-energy density is expected to develop the infinite-volume scaling behavior [54, 93–95, 97]

$$F_{\text{sing}}(u_1, u_2) = |u_2|^{d/y_2} \mathcal{F}_\pm(u_1|u_2|^{-\phi}), \quad (52)$$

in the infinite-volume limit and neglecting subleading corrections, where  $u_1$  and  $u_2$  are the nonlinear scaling fields associated with the two relevant parameters  $r_1$  and  $r_2$ , and  $y_1 > 0$  and  $y_2 > 0$  are the corresponding RG dimensions at the multicritical XY fixed point. The scaling fields  $u_1$  and  $u_2$  are analytic functions of LGW  $\Phi^4$  theory (51), and therefore of the SQI parameters  $g$ ,  $g_e$ , and  $w$ . In the above scaling equation, we neglected corrections to the multicritical behavior due to the irrelevant scaling fields. The functions  $\mathcal{F}_\pm(X)$  apply to the parameter regions in which  $\pm u_2 > 0$ , respectively. The bicritical point is the starting point of three transition lines: two Ising transition lines and one first-order transition line. They follow the scaling equation  $X = u_1|u_2|^{-\phi} = \text{const}$  with a different constant for each transition line. Since  $\phi > 1$ , they are tangent to the line  $u_1 = 0$  (see Fig. 6).

Several field-theoretical and numerical works have determined the exponents  $y_i$  entering the scaling ansatz associated with a bicritical XY point. The leading RG exponents  $y_1$  and  $y_2$  correspond to the RG dimensions of the quadratic spin-2 and spin-0 perturbations at the XY fixed point. The leading RG exponent  $y_1$  is associated with the quadratic spin-two perturbation, whose RG dimension is [102]  $y_1 = 1.76370(12)$ . The second largest exponent is associated with the spin-zero quadratic operator and is directly related to the correlation-length critical exponent at standard XY transitions:  $y_2 = 1/\nu_{xy} = 1.48872(5)$ , obtained using the estimate [101]

<sup>2</sup> Accurate estimates of the critical exponents characterizing the 3D XY universality class can be found in Refs. [54, 96, 98–102], obtained by various theoretical approaches.

$\nu_{xy} = 0.671718(23)$ . Using the above results, we can estimate the crossover exponent  $\phi = y_1/y_2 = 1.1847(1)$ . Other details on the scaling correction exponents, which are related to the spin-4, spin-2, and spin-zero quartic perturbations, respectively, can be found in Refs. [54, 95–97, 102, 103].

Concerning the 2D SQI model, for values of the intercoupling parameter  $w$  within the attraction domain of the multicritical XY fixed point, the multicritical point is located at  $g = g_e = g_{mc}$  (where  $g_{mc}$  is expected to depend on  $w$ ) and the scaling fields entering the scaling Eq. (52) can be identified as  $u_1 \approx g - g_e$  (the first-order transition line departing from the bicritical XY point is expected to run along the line  $u_1 = 0$ ) and  $u_2$  along any other direction (in particular, one may choose  $u_2 \approx g + g_e - 2g_{mc}$ ). Then, when approaching the multicritical point along the line  $u_1 = 0$ , the correlation length is expected to increase as  $\xi \sim u_2^{-\nu_{xy}}$ , while along any other direction it increases as  $\xi \sim u_1^{-1/y_1}$ . Moreover, at the multicritical point, the algebraic decay of the two-point function  $G(\mathbf{x}, \mathbf{y})$  of the longitudinal operator  $\hat{\sigma}_{\mathbf{x}}^{(1)}$  [defined analogously to that of the 1D model, cf. Eq. (9)] is controlled by the 3D XY exponent  $\eta_{xy} = 0.03816(2)$  [101], i.e.,  $G(\mathbf{x}, \mathbf{y}) \sim |\mathbf{x} - \mathbf{y}|^{-1-\eta_{xy}}$ .

## VI. CONCLUSIONS

We have addressed the quantum behavior of a many-body system  $\mathcal{S}$  interacting with a surrounding many-body environment  $\mathcal{E}$ , assuming that the global system is in its ground state. As paradigmatic models, we consider SQI systems, and in particular SQI chains described by Hamiltonian (1) (see Fig. 1). One chain plays the role of the open system  $\mathcal{S}$  under observation, while the other one acts as the environment  $\mathcal{E}$ . The two subsystems interact by means of the Hamiltonian term  $\hat{H}_w$  defined in Eq. (2c), which preserves the  $\mathbb{Z}_2$  symmetries of the SQI subsystems.

We analyze quantum correlations within subsystem  $\mathcal{S}$  and study their dependence on the state of the weakly-coupled complementary part  $\mathcal{E}$  and on the intercoupling strength. We focus on the quantum critical regimes of  $\mathcal{S}$ , showing that the corresponding scaling behaviors crucially depend on whether  $\mathcal{E}$  is itself critical or far from criticality. The most interesting regime arises when both SQI subsystems develop critical correlations. In particular, we consider the case in which the two SQI subsystems are identical, so that the global system is equivalent to the QAT model [41–47], being characterized by an additional  $\mathbb{Z}_2$  interchange symmetry between the subsystems. In this limit, 1D SQI systems develop a peculiar critical line where the length-scale critical exponent  $\nu$  depends on the intercoupling strength  $w$ . Interesting phenomena also occur in higher dimensions. Indeed, we argue that 2D SQI systems display multicritical behaviors characterized by an enlargement of the symmetry of critical modes, from the actual  $\mathbb{Z}_2 \oplus \mathbb{Z}_2$  symmetry to a continuous  $O(2)$

symmetry.

The SQI model studied in this paper substantially differs from the one analyzed in Ref. [36], where the Hamiltonian term is proportional to the product of the longitudinal spin variables [see Eq. (7)], thus breaking the  $\mathbb{Z}_2$  symmetries of the individual SQI systems and leaving only a global residual  $\mathbb{Z}_2$  symmetry. Indeed, substantial differences emerge when comparing the critical behaviors of SQI models that preserve or break the original symmetries of the decoupled subsystems. The results for the SQI systems considered here, together with those reported in Ref. [36], clearly demonstrate that the quantum behavior of  $\mathcal{S}$  (including its coherence properties, phase diagram, and critical behavior) depends strongly on the quantum state of the environment  $\mathcal{E}$ . However, the specific features of the resulting critical behaviors may also depend crucially on the nature of interactions between  $\mathcal{S}$  and  $\mathcal{E}$ , and in particular on which symmetries of the two subsystems are preserved.

Most of the arguments developed here can be straightforwardly extended to cases in which  $\mathcal{S}$  and  $\mathcal{E}$  are of different nature, dimensionality, etc, including situations where  $\mathcal{E}$  is much larger than the observed system  $\mathcal{S}$ . Furthermore, the results obtained for weakly coupled  $d$ -dimensional SQI systems can be extended to the corresponding classical systems, i.e., to coupled  $(d+1)$ -dimensional classical Ising systems with intercoupling that preserve the  $\mathbb{Z}_2$  symmetries of the two subsystems.

The effects of interactions with a bath (environment) on quantum many-body systems have also been investigated using different approaches (see, e.g., Refs. [39, 104–115]). A widely used framework is based on the Lindblad master equation [116, 117], which describes certain classes of dissipative interactions, without keeping track of the full environment dynamics. As shown in various studies within the Lindblad framework, the coupling to the environment generally makes the quantum critical behavior of a closed system unstable [39, 110, 114, 115], similarly to finite-temperature effects. In this context, dissipative couplings act as relevant perturbations that drive the system away from the quantum critical behavior of the isolated model. Alternatives for dissipation are provided by coupling a many-body system to an infinite set of harmonic oscillators (see, e.g., Refs. [104–109]), or to a quantum measurement apparatus (see, e.g., Refs. [118–124]). These types of dissipative interactions are likewise relevant perturbations of the critical behavior of isolated systems and may lead to different forms of dissipation-driven criticality, such as those arising at finite temperature. We emphasize that our setting is substantially different: the global system is isolated and evolves unitarily, rather than being governed by a reduced dissipative dynamics. As a result, our scenario is qualitatively distinct, still allowing for the observation of 1D quantum critical behaviors in systems with short-range interactions.

## Appendix A: Details on the DMRG simulations

To determine the ground-state properties of the two SQI chains under investigation here, we employ a standard two-site DMRG algorithm in its finite-system formulation [40]. We push our DMRG simulations up to  $L = 65$ , corresponding to a total number of  $2L = 130$  sites. To ensure convergence we perform five finite-system back-and-forth sweeps for each parameter set. A crucial parameter in such kind of simulations is the number  $m$  of states (i.e., the bond-link dimension) retained in the renormalization procedure of the enlarged block density matrix. We choose  $m = 100$  for  $L \leq 29$ ,  $m = 120$  for  $33 \leq L \leq 49$ , and  $m = 140$  for  $53 \leq L \leq 65$ , after carefully checking convergence for all the considered system sizes.

The dependence of our results on  $m$  is illustrated in Fig. 7, where we focus on the largest system size  $L = 65$ , for parameters chosen such that the system is close to criticality. To quantify convergence, we consider the symmetric relative difference

$$\Delta_m(O) = \frac{2|O(m) - O(\bar{m})|}{O(m) + O(\bar{m})} \quad (\text{A1})$$

for a given monitored observable  $O > 0$ , comparing results obtained by keeping  $m$  states and  $\bar{m}$  states. In the main frame of the figure, each data point corresponds to  $m$  ranging from 20 to 140, with  $\bar{m} = m - \Delta m$  and  $\Delta m = 10$ . For both the correlation length per site  $R_\xi$  [cf. Eq. (19)] and the ratio  $R_G(1/8, 1/4)$  of the longitudinal correlation function  $G$  at different distances [cf. Eq. (22)], we observe an exponential suppression of

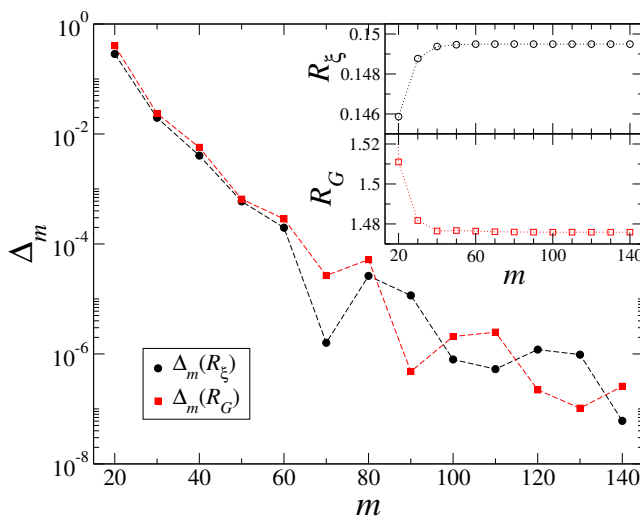


FIG. 7: The symmetric relative difference  $\Delta_m$  for our DMRG calculations of  $R_\xi$  (black) and  $R_G(1/8, 1/4)$  (red), computed by increasing the number of kept states in steps of  $\Delta m = 10$ . The two insets show the explicit dependence of  $R_\xi$  and  $R_G$  on  $m$ . Data are for the 1D QAT model with  $J = J_e = 1$ ,  $g = g_e = 1$ , and  $w = +0.5$ . Here we fix the system size as  $L = 65$ .

$\Delta_m$  with increasing  $m$ . Choosing  $m = 140$  ensures that relative differences remain below  $10^{-6}$ , for all the monitored observables. The two insets clearly show that discrepancies between the results obtained at different and large values of  $m$  are barely visible on the scale of the figure. Likewise, we estimate systematic errors in all the quantities reported in the main text to be smaller than the symbol size.

## Appendix B: Some CFT results for the critical correlations of the quantum Ising chain

Here we focus on a single quantum Ising chain at the critical point with OBC, described by the Hamiltonian (2a) with  $J = g = 1$ . We recall that the particular case of the QAT model for  $w = 0$  corresponds to two decoupled quantum Ising chains. Therefore, in that case, the ground-state two-point function of the quantum Ising chain corresponds to the one defined in Eq. (9).

The 2D Ising universality class can be associated with a CFT with central charge  $c = 1/2$ . CFT provides the asymptotic FSS behavior of the two-point function at the critical point (see, e.g., Refs. [77, 78]). We report some useful formulas for the critical two-point function for  $L \times \infty$  with OBC, i.e., with coordinates  $-\ell \leq x \leq \ell$  and  $y \in \mathbb{R}$ . Thus  $L = 2\ell + 1 \approx 2\ell$  asymptotically in the large- $L$  limit.

Setting  $\vec{r}_i \equiv (x_i, y_i)$ ,  $z_i \equiv x_i + \ell$ ,  $Z_\pm \equiv (z_2 \pm z_1)/L$ ,  $Y \equiv (y_2 - y_1)/L$ , the critical two-point function on a infinite strip of transverse size  $L$  along the  $z$  axis and OBC reads

$$G_{\text{obc}}(\vec{r}_1, \vec{r}_2) = \frac{\pi^{1/4}}{[4L^2 \sin(\pi z_2/L) \sin(\pi z_1/L)]^{1/8}} \quad (\text{B1})$$

$$\times \left[ \frac{|\sin[\pi(Z_+ + iY)/2]|^{1/2}}{|\sin[\pi(Z_- + iY)/2]|^{1/2}} - \frac{|\sin[\pi(Z_- + iY)/2]|^{1/2}}{|\sin[\pi(Z_+ + iY)/2]|^{1/2}} \right]^{1/2}.$$

The fixed-time ground-state two-point function  $G(x, y)$  of the quantum Ising chain at the critical point is obtained by setting  $Y = 0$  in Eq. (B1). Note that one should allow for a multiplicative normalization when comparing  $G_{\text{obc}}$  with lattice computations at the critical point in the large- $L$  limit keeping  $Z_\pm$  and  $Y$  fixed.

This result allows us to exactly compute the universal large- $L$  limit of some RG invariant quantities, such as  $R_\xi$  and  $R_G$  defined in Eqs. (19) and (22), respectively. Using Eq. (B1), we obtain the critical values [53, 125]

$$R_\xi^* \approx 0.159622, \quad R_G^*(1/8, 1/4) \approx 1.358609. \quad (\text{B2})$$

For the Ising chain, we may also consider the connected equal-time two-point function of the operator  $\hat{\sigma}_x^{(3)}$  [cf. Eq. (12)]. CFT computations give [77, 125]

$$F_{\text{obc}}(0, x) \sim \frac{\cos(\pi x/L)}{L^2 \sin^2(\pi x/L)}. \quad (\text{B3})$$

Note that  $F_{\text{obc}}(0, x) \sim x^{-2}$  for  $|x| \ll \ell$ . Therefore, the integral of  $F_{\text{obc}}(0, x)$  with respect to  $x$  is infinite.

One may compare the results for OBC with those with PBC, for which

$$G_{\text{pbc}}(\vec{r}_1, \vec{r}_2) = \frac{(\pi/L)^{1/4}}{|\sin \pi(Z_- + iY)|^{1/4}}. \quad (\text{B4})$$

Again, setting  $Y = 0$ , one obtains the two-point function  $G(x, y)$  at the critical point, from which we obtain  $R_\xi^* \approx 0.187790$  and  $R_G^*(1/8, 1/4) \approx 1.165899$ .

---

[1] W. H. Zurek, Environment-induced superselection rules, *Phys. Rev. D* **26**, 1862 (1982).

[2] W. H. Zurek, Decoherence, einselection, and the quantum origins of the classical, *Rev. Mod. Phys.* **75**, 715 (2003).

[3] M. Gaudin, Diagonalisation d'une classe d'Hamiltoniens de spin, *J. Phys. (Paris)* **37**, 1087 (1976).

[4] N. V. Prokof'ev and P. C. E. Stamp, Theory of the spin bath, *Rep. Prog. Phys.* **63**, 669 (2000).

[5] F. M. Cucchietti, J. P. Paz, and W. H. Zurek, Decoherence from spin environments, *Phys. Rev. A* **72**, 052113 (2005).

[6] H. T. Quan, Z. Song, X. F. Liu, P. Zanardi, and C. P. Sun, Decay of Loschmidt echo enhanced by quantum criticality, *Phys. Rev. Lett.* **96**, 140604 (2006).

[7] D. Rossini, T. Calarco, V. Giovannetti, S. Montangero, and R. Fazio, Decoherence induced by interacting quantum spin baths, *Phys. Rev. A* **75**, 032333 (2007).

[8] F. M. Cucchietti, S. Fernandez-Vidal, and J. P. Paz, Universal decoherence induced by an environmental quantum phase transition, *Phys. Rev. A* **75**, 032333 (2007).

[9] Z.-G. Yuan, P. Zhang, and S.-S. Li, Loschmidt echo and Berry phase of a quantum system coupled to an  $XY$  spin chain: Proximity to a quantum phase transition, *Phys. Rev. A* **75**, 012102 (2007).

[10] C. Cormick and J. P. Paz, Decoherence induced by a dynamic spin environment: The universal regime, *Phys. Rev. A* **77**, 022317 (2008).

[11] W. H. Zurek, Quantum Darwinism, *Nat. Phys.* **5**, 181 (2009).

[12] M. Bortz, S. Eggert, C. Schneider, R. Stübner, and J. Stolze, Dynamics and decoherence in the central spin model using exact methods, *Phys. Rev. B* **82**, 161308(R) (2010).

[13] B. Damski, H. T. Quan, and W. H. Zurek, Critical dynamics of decoherence, *Phys. Rev. A* **83**, 062104 (2011).

[14] B.-B. Wei and R.-B. Liu, Lee-Yang zeros and critical times in decoherence of a probe spin coupled to a bath, *Phys. Rev. Lett.* **109**, 185701 (2012).

[15] T. Nag, U. Divakaran, and A. Dutta, Scaling of the decoherence factor of a qubit coupled to a spin chain driven across quantum critical points, *Phys. Rev. B* **86**, 020401(R) (2012).

[16] S. Suzuki, T. Nag, and A. Dutta, Dynamics of decoherence: Universal scaling of the decoherence factor, *Phys. Rev. A* **93**, 012112 (2016).

[17] R. Jafari, and H. Johannesson, Decoherence from spin environments: Loschmidt echo and quasiparticle excitations, *Phys. Rev. B* **96**, 224302 (2017).

[18] E. Vicari, Decoherence dynamics of qubits coupled to systems at quantum transitions, *Phys. Rev. A* **98**, 052127 (2018).

[19] E. Fiorelli, A. Cuccoli, and P. Verrucchi, Critical slowing down and entanglement protection, *Phys. Rev. A* **100**, 032123 (2019).

[20] D. Rossini and E. Vicari, Scaling of decoherence and energy flow in interacting quantum many-body systems, *Phys. Rev. A* **99**, 052113 (2019).

[21] P. Haikka, J. Goold, S. McEndoo, F. Plastina, and S. Maniscalco, Non-Markovianity, Loschmidt echo, and criticality: A unified picture, *Phys. Rev. A* **85**, 060101(R) (2012).

[22] F. Liu, X. Zhou, and Z.-W. Zhou, Memory effect and non-Markovian dynamics in an open quantum system, *Phys. Rev. A* **99**, 052119 (2019).

[23] J.-X. Liu, H.-L. Shi, Y.-H. Shi, X.-H. Wang, and W.-L. Yang, Entanglement and work extraction in the central-spin quantum battery, *Phys. Rev. B* **104**, 245418 (2021).

[24] H.-Y. Yang, K. Zhang, X.-H. Wang, and H.-L. Shi, Optimal energy storage and collective charging speedup in the central-spin quantum battery, *Phys. Rev. B* **111**, 085410 (2025).

[25] C.-Y. Lai, J.-T. Hung, C.-Y. Mou, and P. Chen, Induced decoherence and entanglement by interacting quantum spin baths, *Phys. Rev. B* **77**, 205419 (2008).

[26] R. Vasseur, S. A. Parameswaran, and J. E. Moore, Quantum revivals and many-body localization, *Phys. Rev. B* **91**, 140202(R) (2015).

[27] C.-Z. Yao and W.-M. Zhang, Probing topological states through the exact non-Markovian decoherence dynamics of a spin coupled to a spin bath in the real-time domain, *Phys. Rev. B* **102**, 035133 (2020).

[28] A. Franchi, D. Rossini, and E. Vicari, Quantum many-body spin rings coupled to ancillary spins: The sunburst quantum Ising model, *Phys. Rev. E* **105**, 054111 (2022).

[29] A. Franchi, D. Rossini, and E. Vicari, Decoherence and energy flow in the sunburst quantum Ising model, *J. Stat. Mech.* (2022) 083103.

[30] A. Mitra and S. C. L. Srivastava, Sunburst quantum Ising model under interaction quench: entanglement and role of initial state coherence, *Phys. Rev. E* **108**, 054114 (2023).

[31] A. Franchi and F. Tarantelli, Liouvillian gap and out-of-equilibrium dynamics of a sunburst Kitaev ring: from local to uniform dissipation, *Phys. Rev. B* **108**, 094114 (2023).

[32] A. Mitra and S. C. L. Srivastava, Sunburst quantum Ising battery, *Phys. Rev. A* **110**, 012227 (2024).

[33] S. Barbarino, J. Yu, P. Zoller, and J. C. Budich, Preparing atomic topological quantum matter by adiabatic nonunitary dynamics, *Phys. Rev. Lett.* **124**, 010401 (2020).

[34] S. Bhattacharjee, S. Bandyopadhyay, D. Sen, and A. Dutta, Bilayer Haldane system: Topological characterization and adiabatic passages connecting Chern phases,

Phys. Rev. B **103**, 224304 (2021).

[35] M. Mannaï, J.-N. Fuchs, F. Piéchon, and S. Haddad, Stacking-induced Chern insulator, Phys. Rev. B **107**, 045117 (2023).

[36] A. Franchi, A. Pelissetto, and E. Vicari, Quantum critical behaviors and decoherence of weakly coupled quantum Ising models within an isolated global system, Phys. Rev. E **107**, 014113 (2023).

[37] S. L. Sondhi, S. M. Girvin, J. P. Carini, and D. Shashar, Continuous quantum phase transitions, Rev. Mod. Phys. **69**, 315 (1997).

[38] S. Sachdev, *Quantum Phase Transitions*, 2nd ed. (Cambridge University Press, Cambridge, 2011).

[39] D. Rossini and E. Vicari, Coherent and dissipative dynamics at quantum phase transitions, Phys. Rep. **936**, 1 (2021).

[40] U. Schollwöck, The density-matrix renormalization group, Rev. Mod. Phys. **77**, 259 (2005).

[41] M. Kohmoto, M. den Nijs, and L. P. Kadanoff, Hamiltonian studies of the  $d = 2$  Ashkin-Teller model, Phys. Rev. B **24**, 5229 (1981).

[42] F. Igloi and J. Solyom, Phase diagram and critical properties of the (1+1)-dimensional Ashkin-Teller model, J. Phys. A **17**, 1531 (1984).

[43] F. C. Alcaraz and J. R. Drugowich de Felicio, Finite size studies of the Ashkin-Teller model, J. Phys. A **17** L651 (1984).

[44] E. Fradkin,  $N$ -Color Ashkin-Teller model in two dimensions: Solution in the large- $N$  limit, Phys. Rev. Lett. **53**, 1967 (1984).

[45] R. Shankar, Ashkin-Teller and Gross-Neveu models: New relations and results, Phys. Rev. Lett. **55**, 453 (1985).

[46] G. von Gehlen and V. Rittenberg, The Ashkin-Teller quantum chain and conformal invariance, J. Phys. A **20**, 227 (1987).

[47] F. C. Alcaraz, M. N. Barber, and M. T. Batchelor, Finite size studies of the Ashkin-Teller model, Ann. Phys. **182**, 280 (1988).

[48] J. Ashkin and E. Teller, Statistics of Two-Dimensional Lattices with Four Components, Phys. Rev. **64**, 178 (1943).

[49] F. Y. Wu and K. Y. Liu, Two phase transitions in the Ashkin-Teller model, J. Phys. C: Solid State Phys. **7**, L181 (1974).

[50] A. Dutta, G. Aeppli, B. K. Chakrabarti, U. Divakaran, T. F. Rosenbaum, and D. Sen, *Quantum phase transitions in transverse field spin models: From statistical physics to quantum information*, (Cambridge University Press, 2015).

[51] P. Pfeuty, The one-dimensional Ising model with a transverse field, Ann. Phys. **57**, 79 (1970).

[52] M. Campostrini, A. Pelissetto, and E. Vicari, Quantum Ising chains with boundary fields, J. Stat. Mech. P11015 (2015).

[53] M. Campostrini, A. Pelissetto, and E. Vicari, Finite-size scaling at quantum transitions, Phys. Rev. B **89**, 094516 (2014).

[54] A. Pelissetto and E. Vicari, Critical phenomena and renormalization group theory, Phys. Rep. **368**, 549 (2002).

[55] M. Caselle, M. Hasenbusch, A. Pelissetto, and E. Vicari, Irrelevant operators in the two-dimensional Ising model, J. Phys. A **35**, 4861 (2002).

[56] M. Baake, G. von Gehlen and V. Rittenberg, Operator content of the Ashkin-Teller quantum chain: superconformal and Zamolodchikov-Fateev invariance: I. Free boundary conditions, J. Phys **20**, L479 (1987); Operator content of the Ashkin-Teller quantum chain, superconformal and Zamolodchikov-Fateev invariance. II. Boundary conditions compatible with the torus, J. Phys. A **20**, L487 (1987).

[57] S. Yang, Modular invariant partition function of the Ashkin-Teller model on the critical line and  $N = 2$  superconformal invariance, Nucl. Phys. B **285**, 183 (1987).

[58] S. Yang and H. Zheng, Superconformal invariance in the two-dimensional Ashkin-Teller model, Nucl. Phys. B **285**, 410 (1987).

[59] M. Yamanaka, Y. Hatsugai, and M. Kohmoto, Phase diagram of the Ashkin-Teller quantum spin chain, Phys. Rev. B **50**, 559 (1994).

[60] M. Yamanaka and M. Kohmoto, Line of continuously varying criticality in the Ashkin-Teller quantum chain, Phys. Rev. B **52**, 1138 (1995).

[61] J. C. Bridgeman, A. O'Brien, S. D. Barlett, and A. C. Doherty, Multiscale entanglement renormalization ansatz for spin chains with continuously varying criticality, Phys. Rev. B **91**, 165129 (2015).

[62] A. O'Brien, S. D. Barlett, A. C. Doherty, and S. T. Flammia, Symmetry-respecting real-space renormalization for the quantum Ashkin-Teller model, Phys. Rev. E **92**, 042163 (2015).

[63] B. E. Lüscher, F. Mila, and N. Chepiga, Critical properties of the quantum Ashkin-Teller chain with chiral perturbations, Phys. Rev. B **108**, 184425 (2023).

[64] Y. Liu, N. Chepiga, Y. Fukusumi, and M. Oshikawa, Boundary critical phenomena in the quantum Ashkin-Teller model, arXiv:2601.16951.

[65] F. Y. Wu, Ashkin-Teller Model as a Vertex Problem, J. Math. Phys. **18**, 611 (1977).

[66] R. J. Baxter, *Exactly solvable models in statistical mechanics*, Academic Press, New York (1982).

[67] E. Domany and E. K. Riedel, Two-dimensional anisotropic  $N$ -vector models, Phys. Rev. B **19**, 5817 (1979).

[68] J. R. Drugowich de Felicio and R. Köberle, Critical exponents of the Ashkin-Teller model, Phys. Rev. B **25**, 511 (1982).

[69] S. Wiseman and E. Domany, A Cluster Method for the Ashkin-Teller Model, Phys. Rev. E **48**, 4080 (1993).

[70] G. Kamieniarz, P. Kozlowski, and R. Dekeyser, Critical Ising lines of the  $d = 2$  Ashkin-Teller model, Phys. Rev. E **55**, 3724 (1997).

[71] G. Delfino and P. Grinza, Universal ratios along a line of critical points. The Ashkin-Teller model, Nucl. Phys. B **682**, 521 (2004).

[72] A. Giuliani and V. Mastropietro, Anomalous universality in the anisotropic Ashkin-Teller model, Commun. Math. Phys. **256**, 681 (2005).

[73] I. Mukherjee and P. K. Mohanty, Hidden superuniversality in systems with continuous variation of critical exponents, Phys. Rev. B **108**, 174417 (2023).

[74] I. Kecoglu and A. N. Berker, Global Ashkin-Teller Phase Diagrams in Two and Three Dimensions: Multicritical Bifurcation versus Double Tricriticality - Endpoint, Physica A **630**, 129248 (2023).

[75] Y. Aoun, M. Dober, and A. Glazman, Phase diagram of the Ashkin-Teller model, Commun. Math. Phys. **405**,

37 (2024).

[76] M. Dober, On antiferromagnetic regimes in the Ashkin-Teller model, *Electron. J. Probab.* **30**, 1 (2025).

[77] C. Itzykson and J. M. Drouffe, *Statistical Field Theory* (Cambridge Univ. Press, Cambridge 1989).

[78] P. Di Francesco, P. Mathieu, and D. Senechal, *Conformal Field Theory* (Springer Verlag, New York, 1997).

[79] N. Khan, P. Sarkar, A. Midya, P. Mandal, and P. K. Mohanty, Continuously Varying Critical Exponents Beyond Weak Universality, *Sci. Rep.* **7**, 45004 (2017).

[80] L. P. Kadanoff, Connections between the critical behavior of the planar model and that of the eight-vertex model, *Phys. Rev. Lett.* **39**, 903 (1977); Multicritical behavior at the Kosterlitz-Thouless critical point, *Ann. Phys.* **120**, 39 (1979).

[81] L. Amico, R. Fazio, A. Osterloh, and V. Vedral, Entanglement in many-body systems, *Rev. Mod. Phys.* **80**, 517 (2008).

[82] S.-J. Gu, Fidelity approach to quantum phase transitions, *Int. J. Mod. Phys. B* **24**, 437 (2010).

[83] D. Braun, G. Adesso, F. Benatti, R. Floreanini, U. Marzolino, M. W. Mitchell, and S. Pirandola, Quantum-enhanced measurements without entanglement, *Rev. Mod. Phys.* **90**, 035006 (2018).

[84] D. Rossini and E. Vicari, Ground-state fidelity at first-order quantum transitions, *Phys. Rev. E* **98**, 062137 (2018).

[85] R. Guida and J. Zinn-Justin, Critical exponents of the  $N$ -vector model, *J. Phys. A* **31**, 8103 (1998).

[86] M. Campostrini, A. Pelissetto, P. Rossi, and E. Vicari, 25th order high-temperature expansion results for three-dimensional Ising-like systems on the simple cubic lattice, *Phys. Rev. E* **65**, 066127 (2002).

[87] M. Hasenbusch, Finite-size scaling study of lattice models in the three-dimensional Ising universality class, *Phys. Rev. B* **82**, 174433 (2010).

[88] F. Kos, D. Poland, D. Simmons-Duffin, and A. Vichi, Precision islands in the Ising and  $O(N)$  models, *J. High Energ. Phys.* 08 (2016) 036.

[89] M. V. Kompaniets and E. Panzer, Minimally subtracted six-loop renormalization of  $\phi^4$ -symmetric theory and critical exponents, *Phys. Rev. D* **96**, 036016 (2017).

[90] A. M. Ferrenberg, J. Xu, and D. P. Landau, Pushing the limits of Monte Carlo simulations for the three-dimensional Ising model, *Phys. Rev. E* **97**, 043301 (2018).

[91] M. Hasenbusch, Restoring isotropy in a three-dimensional lattice model: The Ising universality class, *Phys. Rev. B* **104**, 014426 (2021).

[92] K.-S. Liu and M. E. Fisher, Quantum lattice gas and the existence of a supersolid, *J. Low Temp. Phys.* **10**, 655 (1972).

[93] M. E. Fisher and D. R. Nelson, Spin flop, supersolids, and bicritical and tetracritical points, *Phys. Rev. Lett.* **32**, 1350 (1974).

[94] D. R. Nelson, J. M. Kosterlitz, and M. E. Fisher, Renormalization-group analysis of bicritical and tetracritical points, *Phys. Rev. Lett.* **33**, 813 (1974); J. M. Kosterlitz, D. R. Nelson, and M. E. Fisher, Bicritical and tetracritical points in anisotropic antiferromagnetic systems, *Phys. Rev. B* **13**, 412 (1976).

[95] P. Calabrese, A. Pelissetto, and E. Vicari, Multicritical behavior of  $O(n_1) \oplus O(n_2)$ -symmetric systems, *Phys. Rev. B* **67**, 054505 (2003).

[96] M. Hasenbusch and E. Vicari, Anisotropic perturbations in 3D  $O(N)$  vector models, *Phys. Rev. B* **84**, 125136 (2011).

[97] C. Bonati, A. Pelissetto, and E. Vicari, Multicritical point of the three-dimensional  $\mathbb{Z}_2$  gauge Higgs model, *Phys. Rev. B* **105**, 165138 (2022).

[98] M. Campostrini, M. Hasenbusch, A. Pelissetto, and E. Vicari, Theoretical estimates of the critical exponents of the superfluid transition in  $^4\text{He}$  by lattice methods, *Phys. Rev. B* **74**, 144506 (2006).

[99] S. M. Chester, W. Landry, J. Liu, D. Poland, D. Simmons-Duffin, N. Su, and A. Vichi, Carving out OPE space and precise  $O(2)$  model critical exponents, *J. High Energ. Phys.* **06**, 142 (2020).

[100] C. Bonati, A. Pelissetto, and E. Vicari, Three-dimensional Abelian and non-Abelian gauge Higgs theories, *Phys. Rep.* **1133**, 1 (2025).

[101] M. Hasenbusch, Eliminating leading and subleading corrections to scaling in the three-dimensional XY universality class, *Phys. Rev. B* **112**, 184512 (2025).

[102] M. Hasenbusch, Precision estimates of large charge RG exponents  $Y_q$  in the 3D XY universality class, arXiv:2511.18321.

[103] J. Carmona, A. Pelissetto, and E. Vicari, The  $N$ -component Ginzburg-Landau Hamiltonian with cubic symmetry: a six-loop study, *Phys. Rev. B* **61**, 15136 (2000).

[104] U. Weiss, *Quantum dissipative systems* (World Scientific, Singapore, 2012).

[105] A. O. Caldeira and A. J. Leggett, Quantum tunnelling in a dissipative system, *Ann. Phys.* **149**, 374 (1983).

[106] A. J. Leggett, S. Chakravarty, A. T. Dorsey, M. P. A. Fisher, A. Garg, and W. Zwerger, Dynamics of the dissipative two-state system, *Rev. Mod. Phys.* **59**, 1 (1987); *Rev. Mod. Phys.* **67**, 725 (Erratum).

[107] P. Werner, M. Troyer, and S. Sachdev, Quantum spin chains with site dissipation, *J. Phys. Soc. Jpn. Suppl.* **74**, 67 (2005).

[108] S. Sachdev, P. Werner, and M. Troyer, Universal conductance of nanowires near the superconductor-metal quantum transition, *Phys. Rev. Lett.* **92**, 237003 (2004).

[109] P. Werner, K. Völker, M. Troyer, and S. Chakravarty, Phase diagram and critical exponents of a dissipative Ising spin chain in a transverse magnetic field, *Phys. Rev. Lett.* **94**, 047201 (2005).

[110] S. Yin, P. Mai, and F. Zhong, Nonequilibrium quantum criticality in open systems: The dissipation rate as an additional indispensable scaling variable, *Phys. Rev. B* **89**, 094108 (2014).

[111] O. Alberton, J. Ruhman, E. Berg, and E. Altman, Fate of the One Dimensional Ising Quantum Critical Point Coupled to a Gapless Boson, *Phys. Rev. B* **95**, 075132 (2017).

[112] M. Keck, S. Montangero, G. E. Santoro, R. Fazio, and D. Rossini, Dissipation in adiabatic quantum computers: lessons from an exactly solvable model, *New. J. Phys.* **19**, 113029 (2017).

[113] H. Weisbrich, C. Saussol, W. Belzig, and G. Rastelli, Decoherence in the quantum Ising model with transverse dissipative interaction in the strong coupling regime, *Phys. Rev. A* **98**, 052109 (2018).

[114] D. Nigro, D. Rossini, and E. Vicari, Competing coherent and dissipative dynamics close to quantum criticality, *Phys. Rev. A* **100**, 052108 (2019); D. Rossini

and E. Vicari, Scaling behavior of stationary states arising from dissipation at continuous quantum transitions, *Phys. Rev. B* **100**, 174303 (2019).

[115] D. Rossini and E. Vicari, Dynamic Kibble-Zurek scaling framework for open dissipative many-body systems crossing quantum transitions, *Phys. Rev. Res.* **2**, 023211 (2020).

[116] H.-P. Breuer and F. Petruccione, *The Theory of Open Quantum Systems* (Oxford University Press, New York, 2002).

[117] A. Rivas and S. F. Huelga, *Open Quantum Systems: An Introduction* (SpringerBriefs in Physics, Springer, 2012).

[118] Y. Li, X. Chen, and M. P. A. Fisher, Quantum Zeno effect and the many-body entanglement transition, *Phys. Rev. B* **98**, 205136 (2018).

[119] Y. Li, X. Chen, and M. P. A. Fisher, Measurement-driven entanglement transition in hybrid quantum circuits, *Phys. Rev. B* **100**, 134306 (2019).

[120] X. Cao, A. Tilloy, and A. De Luca, Entanglement in a fermion chain under continuous monitoring, *SciPost Phys.* **7**, 24 (2019).

[121] B. Skinner, J. Ruhman, and A. Nahum, Measurement-induced phase transitions in the dynamics of entanglement, *Phys. Rev. X* **9**, 031009 (2019).

[122] D. Rossini and E. Vicari, Measurement-induced dynamics of many-body systems at quantum criticality, *Phys. Rev. B* **102**, 035119 (2020).

[123] M. Tsitsishvili, D. Poletti, M. Dalmonte, and G. Chiriacò, Measurement induced transitions in non-Markovian free fermion ladders, *SciPost Phys. Core* **7**, 011 (2024).

[124] C. Muzzi, M. Tsitsishvili, and G. Chiriacò, Entanglement enhancement induced by noise in inhomogeneously monitored systems *Phys. Rev. B* **111**, 014312 (2025).

[125] M. Campostrini and E. Vicari, Trap-size scaling in confined-particle systems at quantum transitions, *Phys. Rev. A* **81**, 023606 (2010).